Journal of the European Ceramic Society **17** (1997) 91–100

PII: S0955-2219(96)00081-7
0955-2219/97/$17.00

Scratch Deformation Behaviour of Alumina under a Sharp Indenter

A. K. Mukhopadhyay,[a,*] D. Chakraborty,[b] M. V. Swain[a] & Y.-W. Mai[a]

[a]Department of Mechanical and Mechatronix Engineering University of Sydney, New South Wales 2006, Australia
[b]Central Glass and Ceramic Research Institute, Calcutta 700032, India

(Received 24 April 1995; revised version received 20 April 1996; accepted 3 May 1996)

Abstract

To understand the roles of grain size and a small amount of glassy phase in the abrasive wear mechanisms of brittle ceramics, controlled single-pass scratch experiments were conducted with a Vickers diamond indenter on a range of pure, polycrystalline aluminas of varying grain size (1–25 μm) as well as on a commercial, 10 vol% glass containing alumina (AD90). These tests were made at a constant speed of 0·36 m min^{-1} under a wide range of normal loads, P *(≅ 0·05–20 N). The tangential frictional force, width and depth (and hence wear volume) of the groove all increased with the normal load. The wear volume of 1 μm alumina was about an order of magnitude smaller than those of 5–25 μm grain size pure, polycrystalline aluminas. However, at* P *>10 N the wear volume of AD90 was the smallest of all aluminas examined. These observations of a strong grain size effect and considerable influence of glassy phase in the abrasive wear behaviour of alumina are discussed in terms of residual stress intensity factor and scanning electron microscopic evidence of a wear mechanism controlled predominantly by grain boundary microfracture. © 1996 Elsevier Science Limited.*

1 Introduction

The development of wear-resistant engineering ceramics is essential for their commercial applications in hostile environments involving severe contact stress and temperature. To achieve this goal, a thorough understanding of the roles of basic microstructural parameters such as grain size, glassy phase, density, etc. in controlling the wear of brittle ceramics is very desirable. However, in spite of the wealth of literature, the knowledge base in this regard is far from complete. The subtle, micromechanical contributions from contact stresses, temperature and reactive environment to the wear process often leads to an interesting but complex overall scenario. For example, the wear of pure, polycrystalline alumina (Al_2O_3), a model brittle ceramic, is reported to be a strongly sensitive function of the extent of sub-surface damage,[1] the range of sliding velocity,[2] variations in the amounts of water and relative humidity in the surrounding atmosphere,[3,4] modifications in the near-surface region hardness and, subsequently, the contact stress distributions due to the presence of a hydrated surface layer,[5,6] the chemical nature and volume percentage of a reinforcing second phase such as SiC whiskers,[7] as well as the contact stress and temperature.[8] Grinding is an abrasive wear process similar to a multiple-point multiple-pass scratching phenomenon.[9] Thus. with the philosophy of wear simulation, a significant number of scratch deformation studies on brittle, polycrystalline solids including alumina has been devoted to furthering the understanding of abrasive wear mechanisms.[9–15] Unfortunately, most of these reports involve the applications of merely small loads, e.g. 0·5–5 N, and some slow sliding speeds, e.g. 0·04 μm s^{-1} to 1·0 mm s^{-1}.[9–12]

The abrasive wear mechanisms are proposed to be the formation of vent and chevron cracks,[14] chipping,[16] microfracture[15,17–22] as well as plastic deformation and large-scale brittle failure, depending on the contact stress.[23] Recent work by other researchers[15,18,19] as well as by the present authors and co-workers[20–22] clearly indicates that abrasive wear in a range of engineering ceramics including Al_2O_3 is more due to the fracture and comminution of the nearer to the surface regions, than due to bulk material removal induced by lateral–radial crack interaction as per the commonly accepted view.[24,25] Thus, the abrasive wear mechanisms in ceramics are yet to be established unambiguously.

*Present address: Electroceramics Laboratory, Central Glass and Ceramic Research Institute, Calcutta 700032, India.

The purpose of the present work was to identify the precise roles of grain size *vis-à-vis* small amount of glassy phase in the abrasive wear mechanisms of alumina. Specimens of pure Al_2O_3 were sintered to span the grain size range 1–25 μm and the results compared with those of a commercial, glass-containing AD90 alumina slid against a sharp, pointed, Vickers diamond indenter. This situation simulates more severe contact stress under a wide range of normal loads ($\cong$ 0·05–20 N) at a relatively high sliding speed ($\cong$ 0·36 m min^{-1}).

2 Experimental Work

The pure, polycrystalline alumina samples were prepared from commercially available 99·99% pure alumina powder (Morimura Bros. Inc., Tokyo, Japan). The 10 vol% glassy phase containing alumina, AD90, was obtained from a commercial supplier (M/s Coors Ceramics, Australia). The density measured by the water immersion technique was $\cong$ 90% of theoretical for AD90 and $\cong$ 97·5–98·7% of theoretical for the pure aluminas. The average grain size for AD90 was 2·94 μm. The pure aluminas had grain sizes of ~ 1, 5, 10, 15 and 25 μm.[20–22] All the average grain size data were determined using polished and thermally etched samples with an image analyser. The hardness (H) and fracture toughness (K_{IC}) of all alumina samples were measured by the indentation technique at an applied load of 10 N in a Leitz microhardness tester equipped with a Vickers indenter.

Detailed descriptions of the experimental methods have been given elsewhere.[20–22,26] Briefly, the single-pass scratch experiments were conducted with a reciprocating sliding machine built in our own laboratory. A sharp, pointed, square pyramidal Vickers diamond indenter of tip radius ~ 0·5 μm and apex angle 136°, kept with one leading plane in scratching position, was used on polished, etched and ultrasonically cleaned rectangular test specimens measuring 10 × 6 × 4 mm^3. The friction force was measured using a linear variable displacement transducer (LVDT), the range of normal load was 0·05–20 N and the scratching speed was 0·36 m min^{-1}. Average values of the groove width (B) and groove depth (D) were obtained from at least two experiments by surface profilometry using a Taylor-Hobson Talysurf with a resolution better than ± 1 nm. The wear damage evolution was characterized by scanning electron microscopy (SEM). The cross-sectional examination of the scratch groove was of fractured specimens using SEM and was done by a technique involving notching from the back side prior to fracture. The friction coefficient (f) was evaluated from the the measured values of the tangential force (F) and the normal load (P) as F/P. The wear volume was calculated from the width, depth and length of the scratch assuming a triangular cross-section. The wear rate was estimated from the wear volume data as the volume of material worn per unit load per unit sliding distance. Typical overall average scatter in most of the experimental data was less than 10%.

3 Experimental Results

3.1 Friction and wear characteristics

Figures 1(a)–(h) show the data related to the effects of increasing the normal load (P) and grain size (G) on the scratch characteristics and concerned mechanical properties in the single-pass experiments. In these figures, where applicable, the error bars for the experimental data have been separately included as insets. The tangential force (F), the width (B) and depth (D) of the groove, and hence wear volume (W_v), all increased with the normal load (P), Figs 1(a), (c)–(e). However, the friction coefficient (f) was independent of P [Fig. 1(b)] with a steady state value of $\cong$ 0·6 for all alumina samples. The width and depth of the grooves for the 1 μm and AD90 aluminas were in general smaller than those of the relatively coarse grained materials, Figs 1(c), (d).

The wear volume exhibits a power-law dependence on normal load [Fig. 1(e)]. For sintered alumina, Moore and King also found empirically a power-law dependence between wear volume and normal load.[26] The wear volume of the 1 μm alumina was about an order of magnitude smaller than those of the 5–25 μm grain size aluminas. However, at P >10 N, the wear volume of glass-containing alumina AD90 was the smallest of all the aluminas investigated.

The wear rate (W_R) initially increased with normal load up to 10 or 13 N, prior to a marginal decrease at still higher loads [Fig. 1(f)]. Again, at P > 10 N when all materials are taken together, AD90 alumina exhibits the lowest wear rate. The wear rates found in the present work are similar to those reported by other investigators.[18,27]

The variation in wear volume as a function of grain size is shown in Fig. 1(g). The considerable effect of grain size (G) on wear volume is more prominent at the highest applied normal load of $\cong$ 20 N. In spite of having slightly higher grain size, the superior wear resistance of AD90 is evident from these data.

The hardness (H) of the pure, polycrystalline, sintered alumina samples decreases slightly with

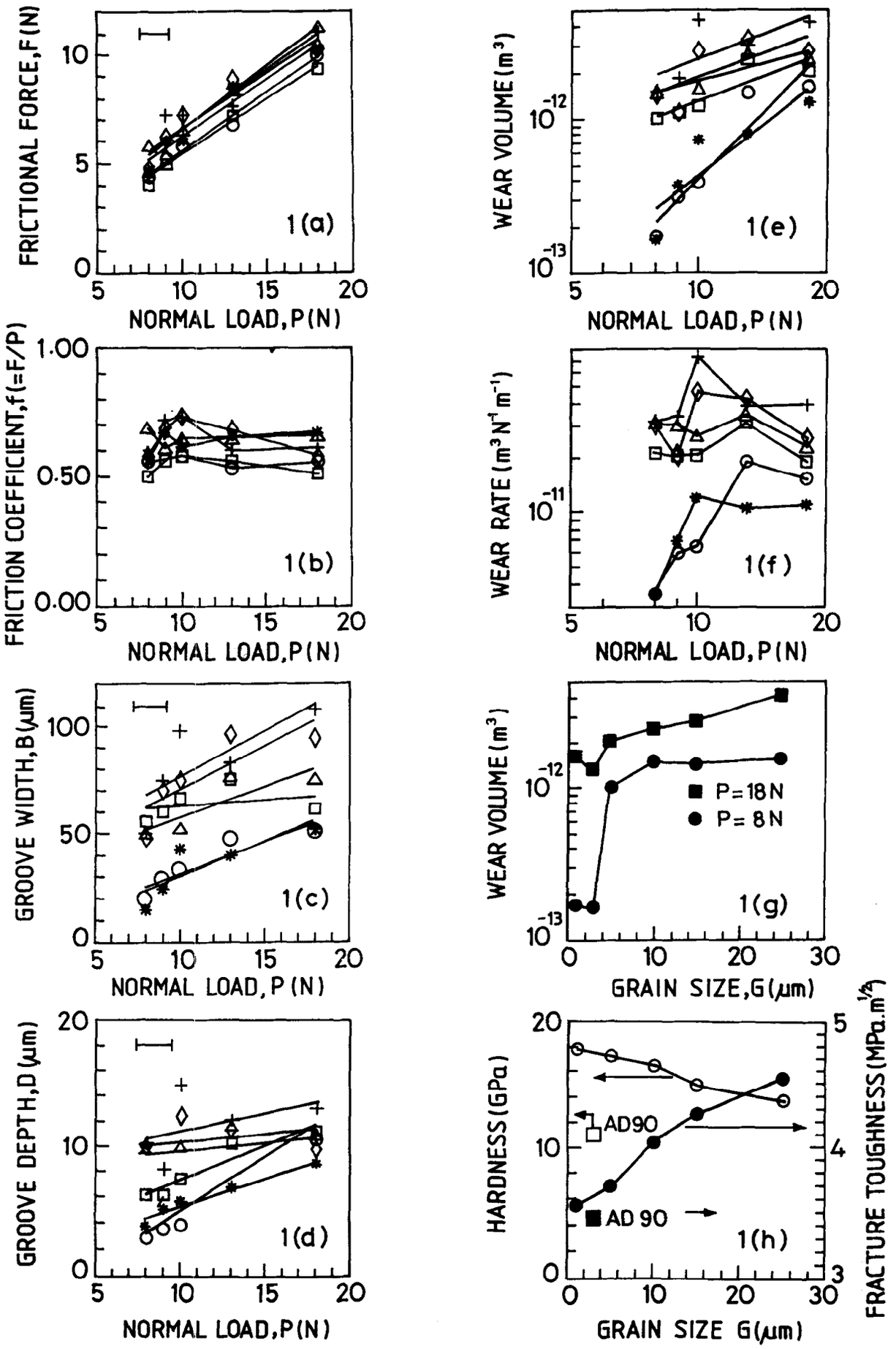

Fig. 1. Normal load (P) versus (a) frictional force (F), (b) friction coefficient (f), (c) scratch groove width (B), (d) scratch groove depth (D), (e) wear volume, (f') wear rate; and grain size (G) versus (g) wear volume and (h) hardness and indentation derived fracture toughness of the present alumina ceramics of different grain sizes [symbols: ○—1 μm, □—5 μm, △—10 μm, ◇—15 μm, +—25 μm pure aluminas and *—2·94 μm glassy alumina (AD90)].

grain size while the fracture toughness (K_{Ic}) shows an opposite trend [Fig. 1(h)]. The glass-containing alumina (AD90) has both hardness and toughness lower than those of the pure, polycrystalline alumina samples.

3.2 Deformation processes

3.2.1 Wear groove characteristics

The microstructure of alumina can exert considerable influence on its wear behaviour.[18,23] Figures 2 (a)–(e) show the microstructure of the five pure alumina samples of different grain size used in the present work. Figure 2(f) shows the microstructure of the glass-containing AD90 alumina.

Figures 3(a)–(d) and 2(f) show scratches made in pure and glass-containing aluminas at very low loads of 0·1 or 0·05 N. At a load of 0·1 N, the scratch grooves in the 1 μm and AD90 alumina exhibit only plastic deformation [Figs 3(a) and 2(f)]. At the same or even smaller load, however, the scratch grooves in the 5 and 25 μm grain size aluminas exhibit additional features of grain boundary microcracking, edge microfracture and even grain pull-out [Figs 3(b)–(d)]. These cracks are of grain facet dimension and originate from near the edge of the track.

The heavier loads of ≅ 8–20 N develop very rough scratch grooves in all the pure, polycrystalline aluminas [Figs 4(a)–(d)] that exhibit extensive intergranular fracture and removal of the scratching track. In sharp contrast to these observations, the deformation is primarily controlled by plastic deformation for the same range of normal load in the AD90 alumina [Figs 4(e), (f)].

3.2.2 Sub-surface damage characteristics

Cross-sectional SEM examination of the wear tracks indicate macrocrack formation in the 1 μm alumina at typical loads of 9 and 13 N [Figs 5(a), (b)]. Even at a high normal load of 13 N there is no evidence of sub-surface lateral crack formation in the 5 μm alumina [Figs 5(c), (d)]. In the coarsest microstructure (e.g. 25 μm) alumina, however, even a small normal load of 0·1 N causes extensive sub-surface damage [Fig. 5(e)]. At heavier loads, e.g. 9 N, the damage is quite complex with a major component of transgranular failure [Fig. 5(f)].

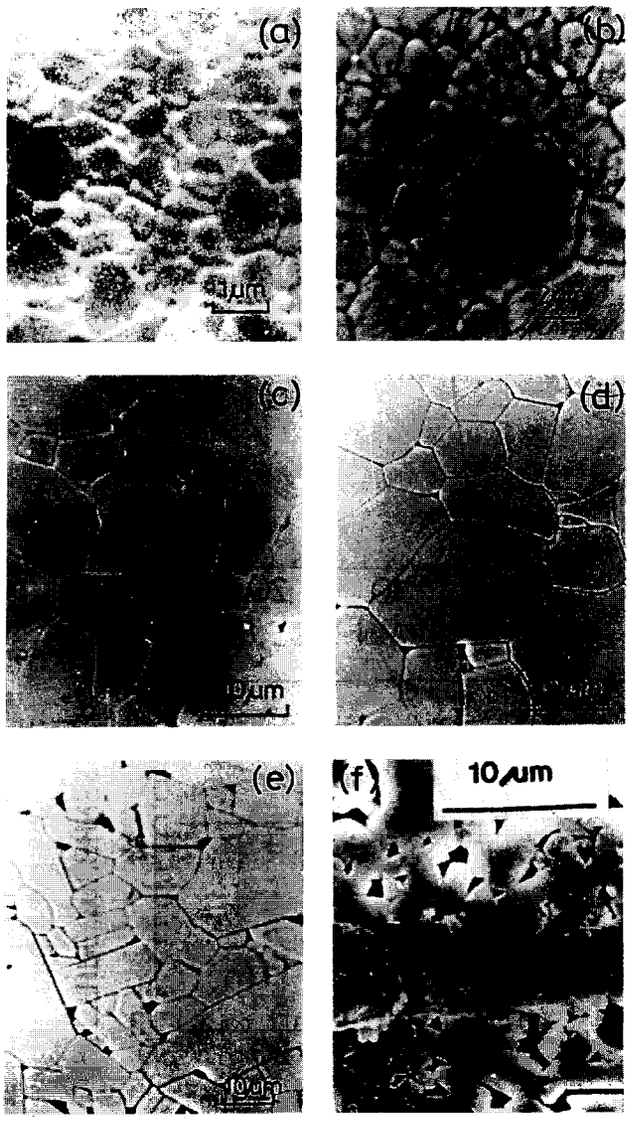

Fig. 2. Polished and thermally etched microstructures of different grain size pure and glass-containing alumina ceramics (a) 1 μm, (b) 5 μm, (c) 10 μm, (d) 15 μm, (e) 25 μm and (f) 2·94 μm (AD90), scratch made at 0·1 N normal load (P).

4 Discussion

4.1 Wear characteristics

The tangential frictional force (F) increases linearly with the applied normal load (P) for all the alumina ceramics investigated [Fig. 1(a)]. A similar observation is reported from low-load, low-speed scratch studies.[10] The friction coefficient, $f (= F/P)$, has a steady-state value of ≅ 0·6, independent of the variations in load or grain size, Fig. 1(b). The data of the present work compare favourably with those of other researchers.[8,10,26]

The increase in groove width (B), depth (D) and hence wear volume (W_v) with the applied normal load, P [Figs 1(c)–(e)], is a reflection of the damage accumulation as the contact stress area and plastic deformation volume are enhanced. Assuming that only the leading plane of the square Vickers indenter is in contact, the experimental data of the groove width [Fig. 1(c)] enable an estimate of the contact stress, σ_c [$= P/(0{\cdot}25B^2)$], in the range from ≅ 6 to 15 GPa in the present aluminas. From the data of Fig. 1(h), an average conservative estimate of the yield stress, $\sigma_y (= H/3)$, is ≅ 5 GPa for the present materials. Thus, nominally, σ_c is » σ_y. However, this is only a simplified estimate. The actual quasi-static stress field, which is

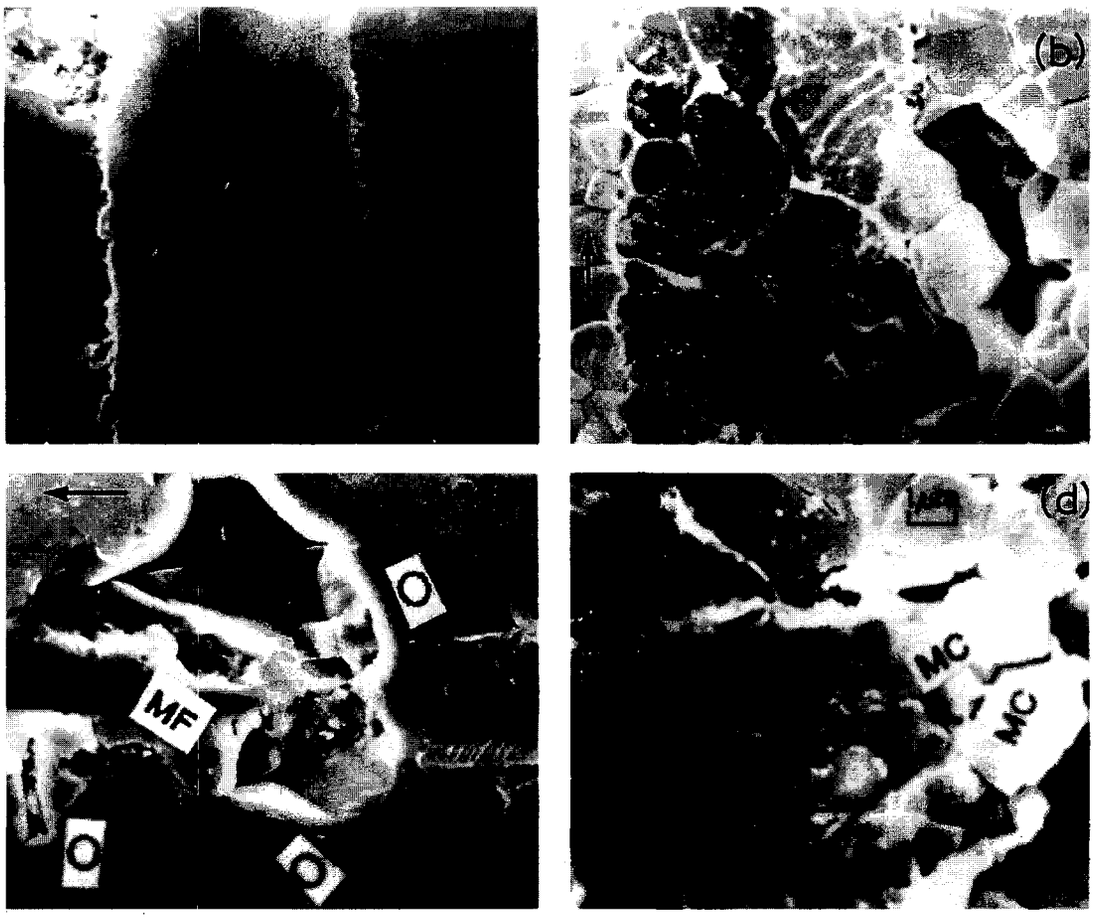

Fig. 3. Observations of plastic deformation, microcracking (MC), microfracture and grain pull-out (O) at $P = 0{\cdot}1$ N in various pure aluminas investigated (arrow indicates sliding direction): (a) 1 μm grain size, (b) 5 μm grain size, (c) 25 μm grain size, (d) 5 μm grain size, $P = 0{\cdot}05$ N.

highly sensitive to normal load,[13] will have, in the presence of the tangential traction, a strong tensile component developed behind the indenter[12] and thus is likely to lower, almost invariably, the critical stress necessary to initiate the grain boundary microfracture[18,19] as evidenced here (Figs 3 and 4).

4.2 Wear rates and mechanisms

The wear volumes exhibit an empirical power-law dependence on the normal load P [Fig. 1(e)], with exponents of 2·90, 1·04, 0·73, 1·01, 1·07 and 2·20 for the 1, 5, 10, 15, 25 μm grain size pure and 2·94 μm grain size AD90 aluminas, respectively. None of these exponent values is in agreement with the theoretical value of 1·125, predicted on the basis of the wear model that assumes the sole dominance of a material removal mechanism based on radial–lateral crack interaction to be operative.[24] Such disagreement is not unexpected because, except for the case of the 1 μm alumina, there is no distinct evidence of lateral crack formation in the sub-surface deformation of the pure aluminas [Figs 5(a)–(f)]. Qualitatively, the observed strong load dependence of W_v is linked to the highly load-sensitive, quasi-static maximum tensile stress development behind the moving indenter.[12,13]

The present observations [Figs 3(b)–(d), 4 and 5], coupled with our previous observations for the wear of the same materials as used here under a blunt indenter[20–22] as well as those of the other investigators,[1,2,15,18,19,23] strongly suggest the presence of alternative wear mechanisms, e.g. removal of a thin surface layer controlled by grain boundary microfracture, in brittle ceramics. Recent observations[28] also indicate that, from among pure as well as glass-containing polycrystalline aluminas of different grain sizes and single-crystal aluminas, the alumina with the highest amount of glassy phase registers the highest grinding force requirement for a given, fixed depth of cut.

The initial increase in wear rate with the normal load [Fig. 1(f)] is expected because the incidence of microcracking about the scratch is enhanced. The marginal reduction in W_R at $P > 10$ or 13 N may be, at least partially, due to the mutually overlapping interaction between the neighbouring scratch grooves caused by the neighbouring asperity distributions on the indenter surface, as suggested by Rice.[23]

Depending on the applied normal load, the wear rate of the fine-grained (1 μm) alumina is about six times to an order of magnitude smaller

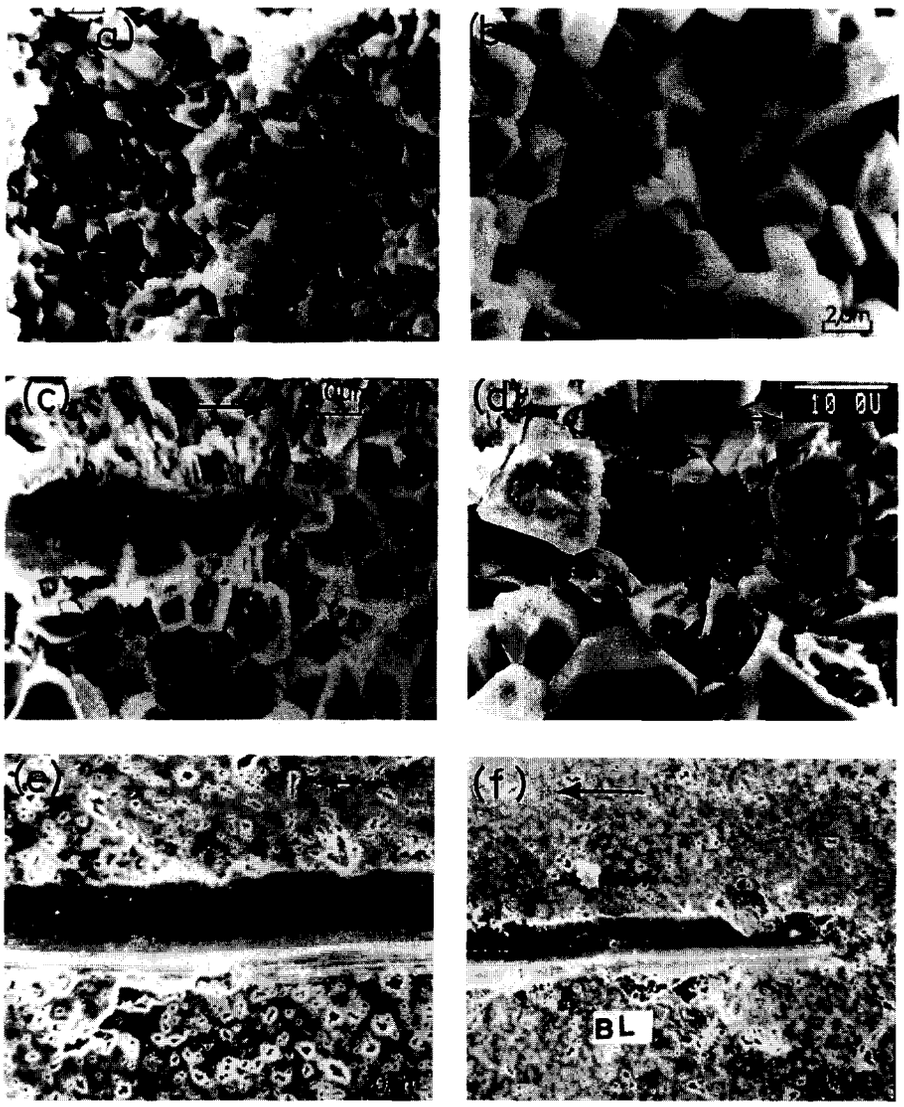

Fig. 4. Observations of scratch groove features at heavier loads in various pure and glassy aluminas studied (arrow indicates sliding direction): (a) intergranular fracture, P = 8 N, 1 μm alumina; (b) inter- and transgranular fracture, P = 8 N, 5 μm alumina; (c) totally or partially crushed grains, dislodged grains with cracked grain boundaries, delamination wear sheet and fine-scale wear debris P = 18 N, 10 μm alumina; (d) additional features of intragranular cracking and deformation band formation, P = 18 N, 25 μm alumina [see near the bottom left corner]; (e), (f) plastic deformation controlled damage and crack blunting (BL) at P = 8 and 18 N, AD90 alumina.

than those of the coarse-grained (5–25 μm) aluminas. This is similar to our earlier observations for the wear of the same materials as used here under a blunt diamond indenter.[20–22] This information suggests that the grain size effect reported here is a genuine material characteristic in the abrasive wear of at least the present pure, polycrystalline alumina ceramics and is independent of the indenter geometry.

At $P > 10$ N, for all materials investigated, the glass-containing alumina AD90 possesses the lowest wear rate (Fig. 1(f)]. This observation can be (at least partially) rationalized in terms of the wear being controlled predominantly by plastic deformation as well as surface crack blunting in AD90 [Figs 4(e), (f)]. For the coarse-grained aluminas the wear rates are in the severe wear regime, i.e. $> 10^{-1}$ m^3 N^{-1} m^{-1},[8] consistent with the observations of a brittle intergranular and/or transgranular fracture controlled process to be dominant in the wear damage evolution [Figs 4(b)–(d)].

The weak inverse grain size dependence of hardness (H) is related to the lack of easy plastic deformability in the relatively coarser microstructures [Fig. 1(h)]. However, the grain coarsening seems to have a beneficial influence on the large crack toughness of the pure aluminas due presumably to the development of an implicit crack growth resistance (R-curve) behaviour as noted by other researchers.[18] Unfortunately, the cracks of grain facet length, which form on the scale of the microstructure during the crucial stage of wear initiation [Figs 3(b)–(d)], are unlikely to benefit from the frictional tractions caused by the grain interlocking which gives rise to the R-curve behaviour in the longer crack systems. This suggestion is

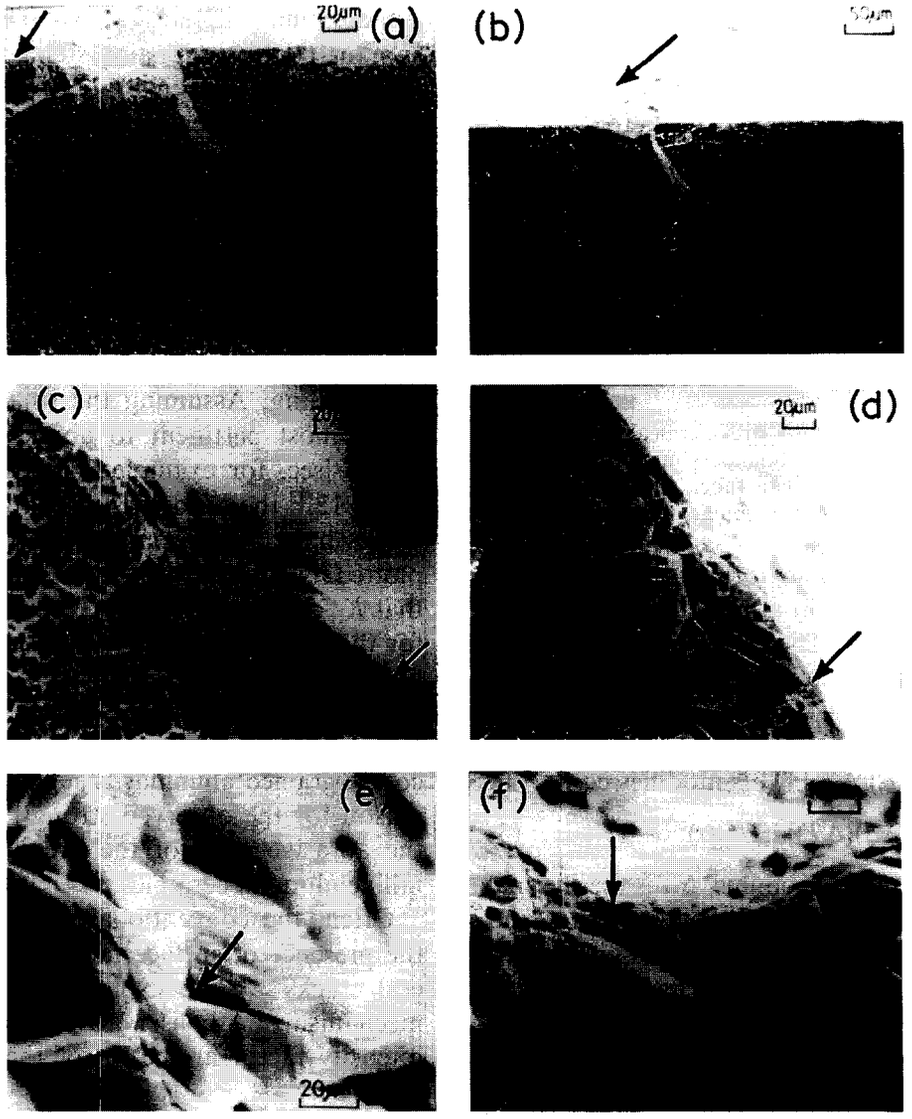

Fig. 5. Cross-sectional SEM observations of sub-surface damage in various pure aluminas (arrow indicates sliding direction): (a), (b) P = 9 and 13 N, 1 μm alumina, lateral cracks present; (c) P = 13 N, 5 μm alumina, notice absence of lateral cracks; (d) magnified view of (c), failure from large grain; (e) P = 0·1 N, 25 μm alumina, notice the presence of deformation bands in a grain just beneath the groove centre and extensive intergranular as well as intragranular cracking in grains near the left off centre to the bottom; (f) P = 9 N, 25 μm alumina, extensive transgranular fracture.

consistent with the observation that the coarse-grained aluminas have much inferior wear resistance to the fine-grained aluminas [Fig. 1(g)].

Notice that AD90 has both the lowest hardness and the lowest K_{1c} of all the aluminas investigated [Fig. 1(h)]. It also has the lowest wear rate at all $P > 10$ N [Fig. 1(f)]. Thus, the present observations of the grain size dependence of wear and toughness are also supportive of the earlier findings[18,28] that the conventional long crack toughness does not necessarily bear a one-to-one correspondence to wear resistance of ceramics, as is often assumed in the modelling of wear.[24]

Interestingly, though neither H nor K_{1c} evaluation points in the proper direction of wear susceptibility, the brittleness index, κ (= K_{1c}^4/H^3) proposed by Lawn and Marshall,[29] does. For example, from the data of Fig. 1(h), the κ values are 27·6, 35·8, 59·9, 100·5, 165·2 and 113·8 μm^2 for the 1, 5, 10, 15, 25 and 2·94 μm grain size pure and glass-containing aluminas, respectively. Thus, at least for the pure aluminas, the material with the highest κ value suffers the largest wear, e.g. 25 μm alumina [Fig. 1(g)], and the 1 μm alumina with the lowest κ value the least.

One important factor that controls the grain-size-dependent wear rate in ceramics is the grain boundary residual stress, σ_r.[1,2,18–23] The wear damage stress (σ_d) necessary to initiate grain boundary microfracture in alumina ceramics is given by:[18]

$$\sigma_d = \sigma_r [(G^*/G)^{0.5} - 1] \quad (1)$$

where G^* is the critical grain size required for spontaneous microfracture. Of the two principal sources of residual stress, e.g. the thermal expansion anisotropy (TEA) stress (σ_t) and the elastic

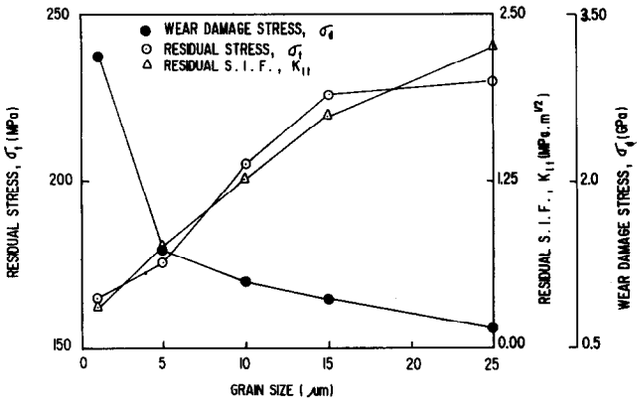

Fig. 6. Variation of residual TEA stress, critical wear damage stress necessary to initiate grain boundary microfractures and residual stress intensity factor as a function of grain size of various pure aluminas.

anisotropy stress (σ_e), the former dominates the latter quite significantly in a non-cubic anisotropic material like alumina. Therefore, expressing $\sigma_r \cong (\sigma_t + \sigma_e) \cong \sigma_t$ modifies eqn (1) to

$$\sigma_d \cong \sigma_t [(G^*/G)^{0.5} - 1] \quad (2)$$

Now, $\sigma_t = [E(\Delta\alpha)(\Delta T)]$. This modifies eqn (2) to

$$\sigma_d \cong [E(\Delta\alpha)(\Delta T)] [(G^*/G)^{0.5} - 1] \quad (3)$$

In eqn (3), E is Youngs' modulus, $\Delta\alpha$ is the thermal expansion coefficient difference between the a and c crystal directions and ΔT is the temperature difference through which the material has been cooled after sintering. Thus, taking $\Delta\alpha = 3{\cdot}5 \times 10^{-7}$ °C^{-1},[30] appropriate E and ΔT values for the present pure, polycrystalline alumina ceramics[20–22] and $G^* = 400$ μm,[18] the TEA stress σ_t and the wear damage stress σ_d estimated from eqn (3) are plotted as a function of grain size in Fig. 6.

Notice that σ_t is lowest for the fine-grained (1 μm) alumina ($\cong$ 160 MPa) and highest ($\cong$ 230 MPa) for the coarsest grained (25 μm) alumina. Similarly, the wear damage stress (σ_d) necessary to initiate grain boundary microfracture is $\cong$ 3·14 GPa for the 1 μm alumina as opposed to a very low value of $\cong$ 0·2 GPa for the 25 μm alumina (Fig. 6). In view of the low σ_d of the 25 μm alumina, if the quasi-static maximum theoretical tensile stress at the wake of the indenter is assumed to be at least of the same order or greater than the nominal contact stress (e.g. $\cong$ 10 GPa at $P = 0{\cdot}1$ N), then the tensile stress should be sufficient to cause grain boundary microfracture in accordance with the SEM observations [Fig. 3(c)]. Therefore, the coarse-grained alumina would undergo grain boundary microfacture more readily than the fine-grained alumina. This suggestion is also consistent with the SEM observations of additional grain boundary microcrack generation in pure, polycrystalline aluminas of $G \geq 5$ μm [Figs 3(b)–(d)] as opposed to the presence of only plastic deformation in 1 μm alumina [Fig. 3(a)] at $P = 0{\cdot}05$–$0{\cdot}1$ N. Further support to this suggestion stems from recent modelling of microcracking due to TEA stress in polycrystalline ceramics as a function of grain size.[31]

Indeed, based on the TEA stress (σ_t) estimation, the residual stress intensity factor (K_{It}) can be expressed as:[20]

$$K_{It} = Y \sigma_t (\pi a)^{0.5} \quad (4)$$

where a is the pre-existing crack length and Y is a geometric factor dependent on the crack shape and loading. Assuming the small crack situation to be most pertinent to abrasive wear in which $a \cong G$ [see, for example, Figs 3(b)–(d), 4(c)] and $Y \cong 1{\cdot}12$,[32] the residual stress intensity factor (K_{It}) values have been estimated from eqn (4) and are plotted as a function of grain size in Fig. 6. Notice that K_{It} assumes the lowest value of $\cong$ 0·3 MPa m$^{0.5}$ for the 1 μm grain size alumina as opposed to the highest value of $\cong$ 2·3 MPa m$^{0.5}$ for the 25 μm grain size alumina. This large difference between the residual stress intensity factors of the fine- and coarse-grained aluminas is suggested to be a major reason for the observed strong grain size effect in the abrasive wear of the present pure, polycrystalline alumina ceramics.

Often, the conventional wear models advocate the presence of surface radial and sub-surface lateral cracks[14,16,33] to explain the material removal mechanism.[24] A conservative estimate of the stress intensity factor at the tip of the median crack is given by:[12]

$$K_m = [m_e P(1 + f^2)^{0.5}]/[\tan \psi (\pi c)^{1.5}] \quad (5)$$

where P is the normal load, f is the corresponding friction coefficient, ψ is the half angle of the indenter ($\cong$ 68°), c is the depth of the median crack and m_e is a multiplicative factor to take care of the modified crack shape. Use of eqn (5) for the median cracks of Figs 5(a) and (b) with the appropriate values of P, f, c and assuming $m_e \cong 1$–4 following Ref. 12, yields estimates of $K_m \cong 3{\cdot}09$ and 3·36 MPa m$^{0.5}$ at $P = 9$ and 13 N, respectively. These values compare favourably with the indentation $K_{Ic} \cong 3{\cdot}55$ MPa m$^{0.5}$, suggesting that the stress intensity factor at the crack tip was $\cong K_{Ic}$ of the material.

From both static spherical indentation induced stress–strain plots[34] and cross-sectional transmission electron microscopic examination of sliding wear specimens[2,18] as well as the conservative estimate of contact stress (σ_c) in the present work, it is evident that stresses developed beneath the contacting asperities are sufficient to cause plastic flow in grains in the near-surface region of the alumina ceramics. This is likely to set up slip or twin systems within the grains [Figs 4(d), 5(e)].

Since the grain boundaries stand as the natural barrier to slip due to twinning or dislocations, they also provide the site for microfracture which is easier to initiate in polycrystalline ceramics. Thus, from theoretical fracture mechanics considerations[35] the pile-up length is directly related to the grain size. Due to the small grain size, the pile-up length in the 1 μm alumina may not be sufficient to nucleate any crack. Thus, with the constraint on the dislocation movement imposed by the small grain size, the high tensile stresses at the wake of the indenter may be accommodated by the formation of sub-surface modified median and lateral cracks [Figs 5(a) and (b)].

In the coarser grained microstructure, the increased pile-up length may provide better means for localized microcracking at grain boundaries [Figs 3(b)–(d), 4(b) and (c)] as well as deformation band formation [Figs 4(d), 5(e)]. The slightly angular orientations of grain boundary cracks to the scratching direction [Fig. 3(d)] may be linked to the simultaneous presence of both tensile and shear stresses.[12,13]

The glass-containing alumina (AD90), on the other hand, undergoes only plastic deformation as the major damage component [Figs 4(e), (f)], resulting in the smallest wear rate of all aluminas [Fig. 1(f)] investigated. This completely different wear mechanism is believed to be linked to the local stress-modifying effects of the grain boundary phase. The lower softening temperature of the glass with its lower modulus reduces the development of the TEA residual stress between the alumina grains. The grain boundary phase, by its relative ease of plastic deformability, may partly relieve the residual stress and thereby cushion the occurrence of microcracks. Further, by partial reduction of the crack driving force, through localized deformation, the grain boundary phase may affect crack blunting [Figs 4(e), (f)] and thereby the wear rate.

The formation of delamination wear sheets [Fig. 4(c)] may be explained by the following hypothesis. Very fine scale wear debris, typically $< 0{\cdot}1$ μm (see, e.g., Fig. 4(d)], produced due to both partial as well as full grain crushing and grain boundary microfracture, are left randomly on the wear track. Already detached from the main wear track, the wear debris assumes locally the thin sheet-like appearance through localized partial compaction and partial thermal densification as it is slid along by the indenter because the local temperature rises in a typical abrasive contact on alumina may be as high as 900–1200°C.[36] The plastic ploughing marks and the grain boundary cracks present on the wear sheet shown in Fig. 4(c) seem to support this mechanism. Further, such high temperatures (e.g. 900–1200°C), especially in the case of the glass-containing alumina, may be sufficient to enable some viscous flow to occur in the grain boundary phase and thereby accommodate the severe plastic ploughing forces without severe intergranular cracking as seen for the pure alumina materials.

5 Conclusions

Based on the experimental results and extensive SEM observations, the following major conclusions can be drawn.

(1) The tangential force of friction (F), the groove width (B) and depth (D), and hence wear volume (W_v), all increase with the normal load (P). A similar trend is shown by the wear rate (W_R) prior to marginal reduction at $P > 10$ or 13 N. The friction coefficient (f) has a steady-state value of $\cong 0{\cdot}6$, independent of grain size (G) and applied normal load.

(2) Among the pure aluminas, the fine-grained (1 μm) alumina has both W_v and W_R smaller by about an order of magnitude than those with $G \geq 5$ μm. This result indicates the presence of a strong grain size effect in the abrasive wear of pure alumina. All aluminas taken together, the AD90 alumina has the least wear volume and rate, suggesting a significant, beneficial influence of the grain boundary glassy phase on the development of resistance to abrasive wear.

(3) At very low normal loads (0·05–0·1 N), plastic ploughing is the major component of deformation in all the aluminas with a secondary mechanism of grain boundary microcrack development in all aluminas with $G \geq 5$ μm.

(4) At heavier loads ($P \cong$ 8–20 N), however, different wear mechanisms prevail for fine- and coarse-grained pure aluminas. Grain boundary microfracture and/or removal of a thin surface layer induced by microcracking emerge(s) as the most general wear mechanism. The present results are, in general, not supportive of a material removal process based on lateral–radial crack interaction. The glass-containing alumina, AD90, undergoes only plastic deformation as the major damage component for the comparable range of applied normal load and thereby attains the smallest wear rate of all aluminas investigated.

Acknowledgements

AKM acknowledges a study leave from the Central Glass & Ceramic Research Institute (CGCRI), Calcutta, India; financial support of the Australian Research Council (ARC) in the form of a Post-doctoral Fellowship tenable at the University of Sydney, Australia; and the keen interest of the Director, CGCRI, in the present work. The authors sincerely thank the Electron Microscope Unit, Sydney University and the Surface Analysis Laboratory, CSIRO Division of Applied Physics, Sydney for their invaluable experimental assistance. The kind co-operation of Dr S. Lathabai, CSIRO Division of Materials Science and Technology, Melbourne, in the preparation of some of the alumina samples used in the present work is gratefully acknowledged. YWM acknowledges the financial support of ARC throughout the period of this project.

References

1. Xu, H. H. K. & Jahanmir, S., Simple techniques for observing sub-surface damage in machining of ceramics. *J. Am. Ceram. Soc.*, **77** (1994) 1388–1390.
2. Cho, S. J., Moon, H., Hockey, B. J. & Hsu, S. M., The transition from mild to severe wear in alumina during sliding. *Acta Metall. Mater.*, **40** (1992) 185–192.
3. Kitaoka, S., Yamaguchi, Y. & Takahashi, Y., Tribological characteristics of α-alumina in high temperature water. *J. Am. Ceram. Soc.*, **75** (1992) 3075–3080.
4. Takadoum, J. & Zsiga, Z., Effect of water vapour in air on friction and wear of Al_2O_3, Si_3N_4 and PSZ sliding on various metals. *J. Mater. Sci. Lett.*, **12** (1993) 791–793.
5. Gee, M. G., Modification of the surface layer of alumina in sliding wear. *Proc. Br. Ceram. Soc.*, **48** (1991) 11–24.
6. Kusy, R. P., Keith, O. & Whitley, J. Q., Coefficient of friction characterisation of surface modified polycrystalline alumina. *J. Am. Ceram. Soc.*, **76** (1993) 336–342.
7. Farmer, S. C., Dellacorte, C. & Brook, P. O., Sliding wear of self matted Al_2O_3–SiC whisker reinforced composites at 23–1200°C. *J. Mater. Sci.*, **28** (1993) 1147–1154.
8. Dong, X., Jahanmir, S. & Hsu, S. M., Tribological characteristics of α-alumina at elevated temperatures. *J. Am. Ceram. Soc.*, **74** (1991) 1036–1044.
9. Broese van Groenou, A., Maan, N. & Veldkamp, J. D. B., Scratching experiments on various ceramic materials. *Phillips Research Report*, **30** (1975) 320–359.
10. Broese van Groenou, A., Maan, N. & Veldkamp, J. D. B., Single point scratches as a basis for understanding grinding and lapping. In *The Science of Ceramic Machining and Surface Finishing, Vol. 2, National Bureau of Standards Special Technical Publication No. 562.* eds B. J. Hockey & R. W. Rice. US Government Printing Office, Washington DC, 1979, pp. 43–60.
11. Veldkamp, J. D. B., Hattu, N. & Snijders, V. A. C., Crack formation during scratching of brittle solids. In *Fracture Mechanics of Ceramics, Vol. 3*, eds R. C. Bradt, D. P. H. Hasselmaan & F. F. Lange. Plenum, New York, 1978, pp. 273–301.
12. Swain, M. V., Microfracture about scratches in brittle solids. *Proc. Royal. Soc.*, **A366** (1979) 575–597.
13. Chen, S. Y., Farris, T. N. & Chandrasekhar, S., Sliding microindentation fracture of brittle materials. *Tribol. Trans.*, **34** (1991) 161–168.
14. Bi, Z., Tokura, H. & Yoshikawa, M., Study of surface cracking of alumina scratched by single point diamond. *J. Mater. Sci.*, **23** (1988) 3214–3224.
15. Ajai, O. O. & Ludema, K. C., Surface damage of structural ceramics: implications for wear modelling. *Wear*, **124** (1988) 237–257.
16. Lawn, B. R., A model for wear of brittle solids under fixed abrasive condition. *Wear*, **33** (1975) 369–372.
17. Swain, M. V., Microscopic observations of abrasive wear of polycrystalline alumina. *Wear*, **35** (1975) 185–189.
18. Cho, S. J., Hockey, B. J., Lawn, B. R. & Bennison, S. J., Grain size and *R*-curve effects in abrasive wear of alumina. *J. Am. Ceram. Soc.*, **72** (1989) 1249–1252.
19. Liu, H. & Fine, M., Modelling of grain size dependent microfracture controlled sliding wear in polycrystalline alumina. *J. Am. Ceram. Soc.*, **76** (1993) 2393–2396.
20. Mukhopadhyay, A. K. & Mai, Y.-W., Grain size effect on abrasive wear mechanisms in alumina ceramics. *Wear*, **162–164** (1993) 258–268.
21. Mukhopadhyay, A. K., Mai, Y.-W. & Lathabai, S., Influence of grain size on deformation characteristics in scratching of alumina ceramics. In *Ceramics — Adding The Value, Vol. 2*, ed. M. J. Bannister. CSIRO Publications, Information Services Branch, Melbourne, 1992, pp. 911–915.
22. Bushby, A. J., Mukhopadhyay, A. K. & Mai, Y.-W., Grain size effect on the mechanism of wear in alumina. In *International Ceramic Monographs, Vol. 1*, eds C. C. Sorrel & A. J. Ruys. Australasian Ceramic Society, Sydney, 1994, pp. 1390–1395.
23. Rice, R. W., Micromechanics of microstructural aspects of ceramic wear. *Ceram. Eng. Sci. Proc.*, **6** (1985) 7–8.
24. Evans, A. G. & Wilshaw, T. R., Quasi-static solid-particle damage in brittle solids – I. observations, analysis and implications. *Acta. Metall.*, **24** (1976) 939–956.
25. Mukhopadhyay, A. K. & Mai, Y.-W., *J. Mater. Sci.*, submitted.
26. Moore, M. A. & King, F. S., Abrasive wear of brittle solids. *Wear*, **60** (1980) 123–140.
27. Gee, M. G., Wear mechanisms for ceramics. *Proc. Br. Ceram. Soc.*, **46** (1990) 287–296.
28. Marshall, D. B., Lawn, B. R. & Cook, R. F., Microstructural effects on grinding of alumina and glass-ceramics. *J. Am. Ceram. Soc.*, **70** (1987) C139.
29. Lawn, B. R. & Marshall, D. B., Hardness, toughness and brittleness: an indentation analysis. *J. Am. Ceram. Soc.*, **62** (1979) 347–350.
30. Schneider, S. J., Jr & Rice, R. W., (eds), *The Science of Ceramic Machining and Surface Finishing, National Bureau of Standards Special Technical Publication No. 348*, US Department of Commerce, Washington, DC, 1972.
31. Sridhar, N., Yang, W., Srolovitz, D. J. & Fuller, E. R. Jr, Microstructural mechanics model of anisotropic thermal expansion induced microcracking. *J. Am. Ceram. Soc.*, **77** (1994) 1123–1128.
32. Tojek, M. M. & Green, D. J., Effect of residual surface stress on the strength distribution of brittle materials. *J. Am. Ceram. Soc.*, **72** (1989) 1885–1890.
33. Smith, S. M. & Scattergood, R. O., Crack shape effects for indentation fracture toughness measurements. *J. Am. Ceram. Soc.*, **75** (1992) 305–315.
34. Lawn, B. R., Padture, N. P., Guiberteau, F. & Cai, H., *Acta Metall. Mater.*, **42** (1994) 1683–1691.
35. Lankford, J., *J. Hard. Mater.*, **2** (1991) 55–59.
36. Cutter, I. A. & McPherson, R., Plastic deformation of Al_2O_3 during abrasion. *J. Am. Ceram. Soc.*, **56** (1973) 66–69.